



ELSEVIER

Available online at www.sciencedirect.com

SCIENCE @ DIRECT®

Earth and Planetary Science Letters 221 (2004) 421–431

EPSL

www.elsevier.com/locate/epsl

Hydrogen incorporation in stishovite at high pressure and symmetric hydrogen bonding in δ -AlOOH

Wendy R. Panero*, Lars P. Stixrude

Department of Geological Sciences, University of Michigan, Ann Arbor, MI 48109, USA

Received 31 October 2003; received in revised form 26 January 2004; accepted 28 January 2004

Abstract

First-principles calculations of stishovite (SiO_2), δ -AlOOH, and stishovite– δ -AlOOH solid solutions reveal that coupled substitutions of Al^{3+} and H^+ for Si^{4+} provide a means for dissolving significant amounts of hydrogen in stishovite under lower-mantle conditions. The enthalpy of solution is positive, decreasing in magnitude with increasing pressure. Combining our results with a model of the configurational entropy we find that the solubility of water in stishovite exceeds 0.3 wt% H_2O at 25 GPa and 1500 K, realistic temperatures for subducting slabs, and that the solubility increases with increasing pressure and temperature. We predict asymmetric hydrogen bonding in the stishovite– δ -AlOOH solid solution that becomes increasingly symmetric with increasing pressure. Our results support the recently predicted symmetric hydrogen bonding in δ -AlOOH, and indicate that symmetric hydrogen bonding may be stable at ambient conditions in this material.

© 2004 Elsevier B.V. All rights reserved.

Keywords: functional theory; stishovite; δ -AlOOH; nominally anhydrous silicates; solid solution

1. Introduction

Nominally anhydrous minerals have the potential to transport and store a significant amount of water in the transition zone and lower mantle [1]. The incorporation of water into silicates is associated with mechanical weakening [2] and affects seismic wave anisotropy and attenuation [3]. Even small concentrations of water in mantle minerals can serve as a significant volatile reservoir in the planet [4].

Understanding the mechanism of hydrogen incorporation in silicates at mantle conditions is important because many nominally anhydrous minerals show increased hydrogen solubility with increasing pressure. For instance, hydrogen solubility in pyrope garnet increases by a factor of four between 0 and 10 GPa [5], and hydrogen solubility in olivine increases by a similar amount between just 50 and 300 MPa [6]. The solubility of hydrogen in olivine composition also increases dramatically as it undergoes polymorphic phase transitions to wasdleyite and ringwoodite (e.g. [7]).

Less is known about the solubility of water in materials with octahedrally coordinated silicon. Stishovite (rutile-structured SiO_2) forms in sub-

* Corresponding author. Tel.: +1-736-615-4074;
Fax: +1-734-763-4690.
E-mail address: wpanero@umich.edu (W.R. Panero).

ducting basalt at depths greater than 300 km [8] and serves as a model for lower-mantle silicates with octahedrally coordinated silicon. With only a few likely arrangements of hydrogen in this relatively simple structure, stishovite is an ideal phase to consider when addressing mechanisms for water dissolution in high-pressure silicate phases. Moreover, stishovite is a chemically simple system that forms as a nearly pure phase in nominally anhydrous compositions, dissolving only small amounts of aluminum [9–11].

Experiments have shown that measurable amounts of H may be dissolved in the stishovite structure and that this mineral may be a major carrier of water to greater depths [12,13]. H solubility is found to be enhanced by the presence of aluminum, present in the lower mantle and subducting slabs as a minor component [12]. On the basis of these observations, Panero et al. [13] proposed a coupled substitution mechanism for the incorporation of hydrogen in stishovite: $\text{Si}^{4+} = \text{Al}^{3+} + \text{H}^+$. This mechanism is also suggested by the structural similarity of SiO_2 stishovite and its high-pressure CaCl_2 -structured polymorph and the CaCl_2 -structure high-pressure polymorph of AlOOH [14]. Our goal is to test the hypothesized solubility mechanism, to elucidate the structural environment of H in stishovite and the influence of hydrogen bonding on elasticity, and to predict the effect of pressure and temperature on H solubility in stishovite.

With this relatively simple nominally anhydrous silicate system, first-principles calculations can explore fundamental issues regarding the nature of hydrogen bonding at high pressure. While little is known about the fundamentals of hydrogen bonding at high pressure, several lines of evidence indicate that it may be qualitatively different from low-pressure hydrogen bonding. At low pressure, hydrogen bonds ($\text{O}-\text{H}\cdots\text{O}$) consist of a shorter, stronger O–H bond ($\sim 0.9\text{--}1.1$ Å) and a longer, weaker $\text{O}\cdots\text{H}$ bond. Compression experiments on H_2O -ice have revealed a pressure induced transition to a qualitatively different form of hydrogen bonding in which the two H–O distances are equal and the hydrogen bond is referred to as being symmetric. Ice retains its molecular identity up to about 60–70 GPa, at which point ice

VII transforms to non-molecular, symmetrically bonded ice X without significant rearrangement of the oxygen lattice [15]. This transition is associated with an increase in bulk modulus at the transition pressure, indicating that the type of hydrogen bonding can affect the elasticity of materials greatly.

We describe first principles calculations of stishovite and a dilute stishovite– AlOOH solid solution that test the proposed coupled substitution of $\text{Si}^{4+} + \text{O}^{2-} = \text{Al}^{3+} + \text{OH}^-$. Computations of the properties of the end-member δ - AlOOH composition allow us to test the reliability of our theoretical methods for describing the physics of hydrogen bonding and to place our computations of defect structures into the context of solution thermodynamics, providing for predictions of hydrogen solubility in stishovite as a function of pressure and temperature.

2. Methods

2.1. Solubility of hydrogen into stishovite

The inter-solubility of two end-member compositions is controlled by the enthalpy and entropy of the solution: if the enthalpy of solution is negative, solid solution is complete. If the enthalpy of solution is positive (unfavorable), then solid solution is in general limited and temperature dependent, typically increasing with increasing temperature through the entropic contributions to the free energy of the solution. The equilibrium solubility is given by the minimum of the Gibbs free energy of solution ΔG at a given temperature and pressure [16]:

$$\Delta G(x, P, T) = \Delta H(x, P, T) - T\Delta S(x, P, T) \quad (1)$$

where x is the extent of solid solution, and ΔH and ΔS are the enthalpy and entropy of solution, respectively. In this study, we compute ΔH from first principles under static conditions (0 K) and assume that ΔH does not depend on temperature, i.e. that the entropy of solution is ideal. We restrict our attention to the dilute solution limit by computing ΔH for one dilute composition and assuming that ΔH varies linearly with composi-

tion over the range of interest; we test this assumption with additional first principles calculations described below.

The entropy of solution has two sources: mixing of Al and Si on the octahedral sites and the multiplicity of symmetrically equivalent locations of the H atoms in the vicinity of the Al octahedron. We find that for each Al+H substitution, there are four possible H positions of identical energy. The configurational entropy, ΔS , is derived directly from the definition:

$$\Delta S = k_B \ln(\Omega_N) \quad (2)$$

where k_B is Boltzmann's constant. The number of possible configurations, Ω , of t Al+H coupled substitutions in a total of N sites is:

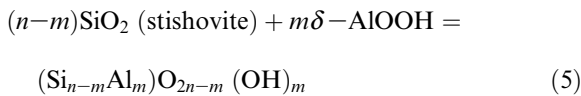
$$\Omega_N(t) = 4^t \frac{N!}{t!(N-t)!} \quad (3)$$

By the Stirling approximation Eq. 2 can be rewritten as:

$$\Delta S \cong -R[(1-x) \ln(1-x) + x \ln x] + Rx \ln(4) \quad (4)$$

where x is the mole fraction of aluminum: t/N . The solubility is found by solving $d\Delta G/dx = 0$.

Here we calculate the enthalpy of solution from the reaction:



The size of our computational supercell corresponds to $n=24$, and we investigate structures with one and two defects ($m=1,2$). We argue below that the enthalpy of solution per defect is not sensitive to the value of n , i.e. we are essentially in the dilute limit.

2.2. Density functional theory calculations

We performed first principles calculations based on density functional theory within the local density (LDA) and pseudopotential approximations of fully relaxed, static (0 K) structures of stishovite, δ -AlOOH, and solid solutions of intermediate composition using the Vienna ab-initio simulation package (VASP) [17–20]. All computations were based on a $2 \times 2 \times 3$ supercell containing 12

primitive unit cells, and from 72 (silica) to 96 (AlOOH) atoms. Tests showed that a $1 \times 1 \times 1$ k -point mesh and a cutoff energy of 600 eV were sufficient to converge the total energy to within 10 meV and the equilibrium volume to within 0.1%. In order to test the effects of the assumed form of the exchange-correlation functional, we also performed calculations based on the generalized gradient approximation (GGA).

For silica, we relaxed SiO_2 in the rutile structure ($P4_2/mnm$) at pressures less than 45 GPa, and in PI symmetry at higher pressures. Relaxation of the structure above 45 GPa results in the CaCl_2 structure ($Pnmm$) in agreement with experiment and previous theory [21,22].

For δ -AlOOH structure relaxations were initiated with the anhydrous sublattice in the CaCl_2 structure ($Pnmm$) as found experimentally [23], but with H atoms on general positions, which lowered the initial symmetry to PI . H atoms were placed near, but not on half of the 4a sites [24] (Fig. 1c), and then all atom positions were fully optimized.

Calculations of stishovite- δ -AlOOH solid solutions were performed with one Al+H for Si substitution per supercell, yielding a composition of 4.2 mol% Al and H (3.5 wt% Al_2O_3 ; 0.6 wt% H_2O), in a 73-atom supercell. We initiated relaxations with the H in several different positions, finding that bonding to the apical oxygen of the Al octahedron was most stable (Fig. 1b). We note that the composition is likely much more water rich than expected for stishovite in the mantle [13]. However, these calculations are in the dilute (non-interacting) limit as shown by the diminishing lattice strain associated with the defect, which essentially vanishes at distances less than half the relevant translational repeat unit (Fig. 1b). We did not consider the possibility of water molecules because infrared spectra show no evidence of the water bending mode [12].

2.3. Corrections to static calculations

Our calculations are static: they do not include the effects of lattice vibrations. In order to compare more directly with room temperature experimental observations, we have estimated the effects of lattice vibrations based on a simple

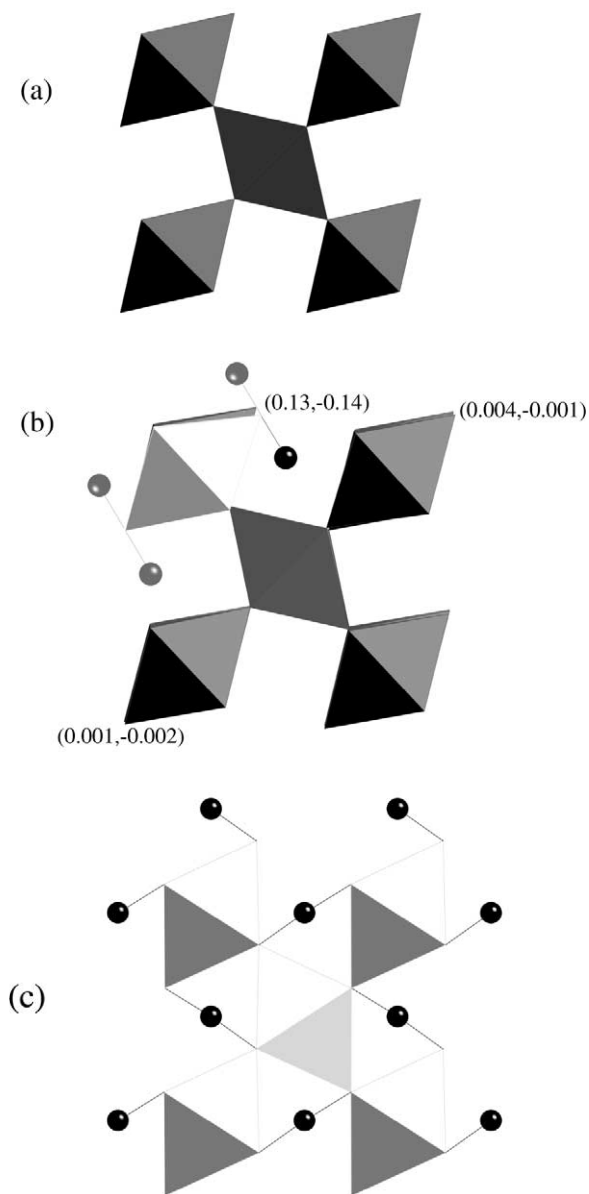


Fig. 1. Calculated structure of (a) stishovite, (b) stishovite with 4.2 mol% $\text{Al}^{3+}+\text{H}^+$, and (c) $\delta\text{-AlOOH}$ at zero pressure in the (110) plane. Light gray octahedra are AlO_6 and dark gray octahedra are SiO_6 , and black spheres are hydrogen atoms. Note the local distortion of the oxygen lattice in the solid solution (b) where the numbers represent the (x,y) displacement in angstroms of the oxygen atom in the same plane as the hydrogen interstitial. The gray spheres in (b) show the other three energetically equivalent positions for the hydrogen interstitial.

model of the vibrational density of states. We consider the pressure due to zero-point motion, P_{zp} and the thermal pressure, P_{th} at 300 K [25].

The zero-point energy, E_{zp} is:

$$E_{zp} = \sum_i^{3n} \frac{\hbar}{2} \omega_i = 3n\hbar\omega/2 \quad (6)$$

where \hbar is Planck's constant divided by 2π , $3n$ is the number of modes per formula unit, ω_i is the vibrational frequency of each mode, and ω is the mean frequency. The zero-point pressure is given by the volume derivative:

$$P_{zp} = -\left(\frac{\partial E_{zp}}{\partial V}\right)_T = -\frac{3n\hbar}{2} \frac{\partial \omega}{\partial V} \quad (7)$$

We adopt the Debye model of the vibrational density of states. The Debye temperature, Θ_D , is related to the mean vibrational frequency as:

$$\frac{3}{4}k_B\Theta_D = \hbar\omega \quad (8)$$

where k_B is the Boltzmann's constant. Defining the Grüneisen parameter:

$$\gamma = \frac{\partial \ln \omega}{\partial \ln V} = -\frac{V}{\omega} \frac{\partial \omega}{\partial V} \quad (9)$$

the zero-point pressure is:

$$P_{zp} = \frac{9n\gamma}{8} \frac{k_B\Theta_D}{V} \quad (10)$$

For stishovite, with $\Theta_D = 1140$ K, $\gamma = 1.35$ [26], and a volume per atom $V/n = 7.67$ Å³, the zero-point pressure correction is 3.1 GPa.

In the Debye approximation, the thermal energy is:

$$E_{th} = 9nk_B T (T/\Theta_D)^3 \int_0^{\Theta_D/T} \frac{x^3}{e^x - 1} dx \quad (11)$$

and the thermal pressure is:

$$P_{th} = -\left(\frac{\partial E_{th}}{\partial V}\right)_T = \frac{\gamma}{V} E_{th} \quad (12)$$

Assuming Θ_D and γ as above, we find that the thermal pressure is 0.6 GPa for a total pressure correction to static results of 3.7 GPa.

For the solid solution, thermal parameters are taken to be equal to those of pure stishovite. Assuming thermal parameters for corundum as an

estimate for δ -AlOOH ($\Theta_D = 1034$ K; $\gamma = 1.32$ [27]), the total correction at zero-pressure is 4.2 GPa, where 0.15 GPa comes from including the effects of the OH vibration to the thermal energy as an Einstein oscillator, taken as 2748 cm⁻¹ [14].

3. Results

3.1. Stishovite

Our results for the structure of stishovite are within 0.4% of those of Karki et al. [22], where slight differences likely reflect the use of a different set of pseudopotentials. Our two highest pressure relaxations (56 and 64 GPa) yield the CaCl₂ structure, and are in excellent agreement with previously calculated oxygen internal coordinates at those pressures [22]. Comparison with experiment is also excellent: at pressures below 47 GPa, temperature-corrected models reproduce volumes to within 0.9% and oxygen positions in rutile-struc-

Table 1

Static structural parameters of stishovite, δ -AlOOH and solid solutions

	Stishovite	Solid solution	δ -AlOOH
0 GPa			
<i>a</i>	4.1413 Å	4.1427 Å	4.6296 Å
<i>b</i>			4.1155 Å
<i>c</i>	2.6718 Å	2.6752 Å	2.8127 Å
<i>V</i>	45.782 Å ³	45.987 Å ³	53.591 Å ³
<i>x</i>	0.3055		0.3518
<i>y</i>			0.2412
O–H		1.037 Å	1.210 Å
H...O		1.694 Å	1.210 Å
OHO angle		177.1°	180°
60 GPa			
<i>a</i>	4.0009 Å	4.0254 Å	4.3577 Å
<i>b</i>	3.8594 Å	3.8621 Å	3.9114 Å
<i>c</i>	2.5693 Å	2.5974 Å	2.6263 Å
<i>V</i>	39.673 Å ³	40.380 Å ³	44.765 Å ³
<i>x</i>	0.3213		0.3457
<i>y</i>	0.2820		0.2422
O–H		1.112 Å	1.16 Å
H...O		1.241 Å	1.16 Å
OHO angle		163.5°	180°

Solid solution lattice parameters are calculated assuming randomized substitutions as in Fig. 1b, and zero-pressure volumes are fit to a finite strain curve of energy vs. $V^{-2/3}$.

Table 2
Structural parameters corrected to 300 K compared to available experimental values

	Stishovite		δ -AlOOH	
	Calculated	Measured	Calculated	Measured
0 GPa				
<i>a</i>	4.153 Å	4.180 Å ^a	4.657 Å	4.713 Å ^b
<i>b</i>			4.141 Å	4.224 Å
<i>c</i>	2.679 Å	2.667 Å	2.829 Å	2.833 Å
<i>V</i>	46.148 Å ³	46.591 Å ³	54.553 Å ³	56.395 Å ³

^a Ross et al., 1990 [28].

^b Suzuki et al., 2000 [23].

tured SiO₂ within 0.3% of experimental values [28] (Tables 1–3; Figs. 1a and 2a).

3.2. δ -AlOOH

Our calculations show that hydrogen forms symmetric hydrogen along $\langle 110 \rangle$ at all non-negative pressures (Fig. 1c; Table 1). Calculations at negative pressures show that hydrogen bonding first becomes asymmetric upon expansion at -8 GPa. Our results disagree with those of Tsuchiya et al. [29] who found asymmetric hydrogen bonding at positive pressures, up to 28 GPa. The reason for this discrepancy is likely the different ap-

Table 3
Equations of state for stishovite, δ -AlOOH and solid solutions

	K_0 (GPa)	K_0'
VASP:		
Stishovite	320.0	3.72
	312.2 (2.1)	4.8 (fixed)
Stish+4.2 mol% Al ³⁺ +H ⁺	314.1	3.76
	303.7 (7.9)	4.8 (fixed)
δ -AlOOH	230.4 (3.2)	4.1 (2)
Experiment (300 K):		
Stishovite ^a	312.9 (3.4)	4.8 (0.2)
Stishovite+2.1 wt% Al ₂ O ₃ ^b	278.4 (9)	3.7 (1.3)
δ -AlOOH ^c	188.0 (5.8)	9.4 (1.0)
	217.8 (1.9)	4 (fixed)

^a Panero et al., 2003 [10].

^b Reanalyzed from Ono et al., 2002 [11] (H content is unmeasured).

^c Reanalyzed from Vanpeteghem et al., 2002 [30].

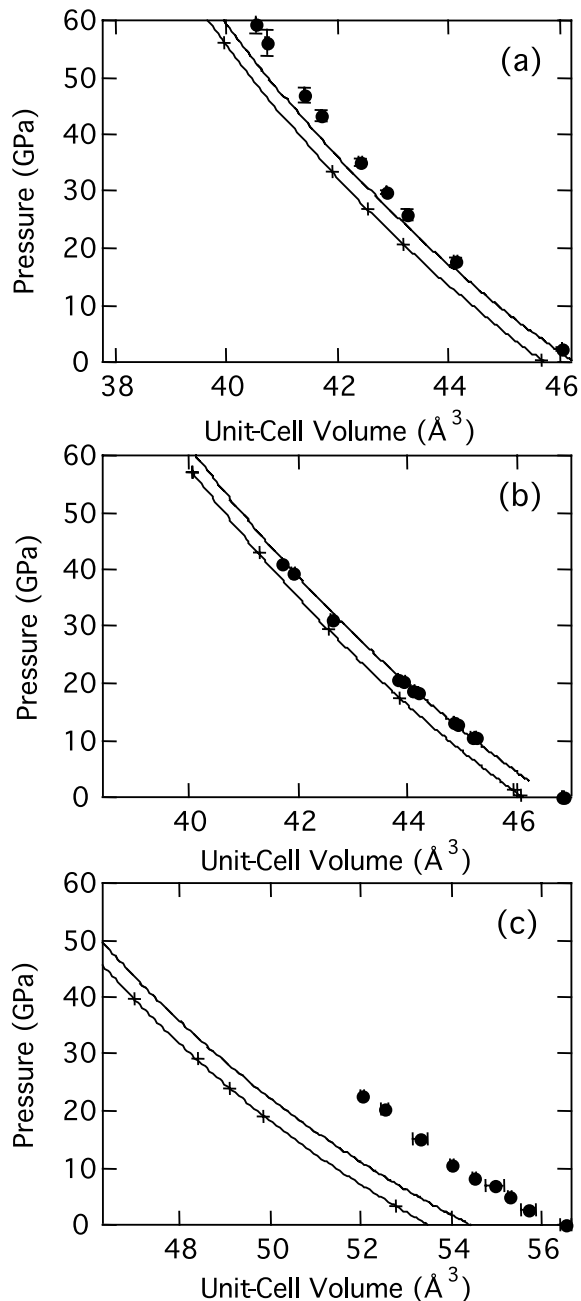


Fig. 2. Pressure–volume relationships for the three structures modeled. Solid line is the fit to the calculated static points (crosses), dashed line is corrected to 300 K, and circles are experimental points for (a) stishovite [10], (b) 2.4 mol% (2.1 wt%) Al in stishovite [11], and (c) δ -AlOOH [30]. The volume axis is such that the range of volumes (V/V_0) is equivalent.

proximations to the exchange-correlation potential used in the two studies: whereas we used LDA, Tsuchiya et al. [29] used GGA. We tested this hypothesis by performing a series of GGA calculations. We found that at the same volume, GGA and LDA predicted nearly identical structures, the most significant difference being in the calculated pressure, which was higher by 8 GPa for GGA than for LDA. We found that the two sets of calculations agree in the range of volume over which asymmetric hydrogen bonding occurs, but not in pressure.

Several lines of evidence support our prediction of symmetric hydrogen bonding in δ -AlOOH at ambient and higher pressures. The non-bonded O–O distance in δ -AlOOH is very short: 2.42 Å, similar to the O–O distance in symmetrically bonded Ice X (2.4 Å) at its lowest pressure of stability [15]. Powder neutron diffraction shows that β -CrOOH may also exhibit symmetric hydrogen bonds although fits to the data cannot distinguish between symmetric and asymmetric hydrogen bonding [24]; the O–O distance in β -CrOOH is 2.472(3) Å. Raman spectra reported in Ohtani et al. [14] show a broad band at 2748 cm⁻¹ that may be due to OH bond stretching. Such a low frequency is expected for symmetric hydrogen bonds, whereas the hydroxyl of asymmetric hydrogen bonds generally has a higher stretching frequency. Finally, we make the testable prediction that since the hydrogen bond is symmetric, the hydroxyl stretching frequency should increase with increasing pressure.

Structural and compressional experimental data agree with our temperature-corrected theoretical results to within 3.3% (Tables 2–3). Calculated linear compressibilities further support our prediction of symmetric hydrogen bonding. We find that the *c*-axis is most compressible, in agreement with experimental static-compression data [30] and with the calculations of Tsuchiya et al. [29] over the pressure interval that those authors find symmetric bonding. The greater compressibility along the *c*-axis reflects the orientation of the O–H–O bond along $\langle 110 \rangle$, which stiffens the *a*- and *b*-axes with respect to the *c*-axis. This is in contrast to stishovite where the *c*-axis is significantly stiffer than the *a*-axis [28]. In the asymmet-

ric bonding regime at pressures less than –8 GPa, we find a transition in the trend of compressibility where the *c*-axis becomes the stiff axis.

3.3. 4.2 mol % solid solution

The inclusion of 4.2 mol% aluminum and hydrogen for silicon in the stishovite structure results in a greater zero-pressure volume (0.4%) and a bulk modulus that is indistinguishable from stishovite.

We found that hydrogen was most stable when bonded to the apical oxygen of the Al-octahedron, with the hydroxyl bond along $\langle 110 \rangle$ and co-planar with Al (Fig. 1b). The location of the hydrogen is consistent with predictions made from charge density analyses [31] and the experimental observation that the OH bond stretch absorbs light polarized normal to the *c*-axis [12]. We found that H bonded instead to one of the equatorial oxygens of the Al-octahedron was mechanically unstable and relaxation returned the H to the apical position. When hydrogen was not directly associated with an AlO₆ octahedron, the energy cost was significant. A configuration in which the H was bonded to an oxygen of a Si-octahedron was higher in energy by more than 1 eV per hydrogen. The energy costs are greater for locating the hydrogen within the AlO₆ octahedron, about 5 eV greater than the most stable arrangement reported here.

The Al-octahedron is rotated with respect to the Si-octahedra by an amount that corresponds to fractional coordinates of the oxygens of $x=0.337$ and $y=0.282$ in terms of the CaCl₂ structure (Fig. 1b). This rotation is identical in sense, though slightly less in magnitude to that which relates the octahedra in the stishovite and the δ -AlOOH structures. The relatively short O–O distance and correspondingly long O–H distance in the stishovite– δ -AlOOH solid solution (Table 1) would lead one to expect a low OH stretching frequency compared to other nominally anhydrous minerals [32], consistent with the value of 3111 cm⁻¹ observed by Pawley et al. [12]. Because the bond is asymmetric, we anticipate that the vibrational frequency should decrease with increasing pressure (mode Grüneisen parameter

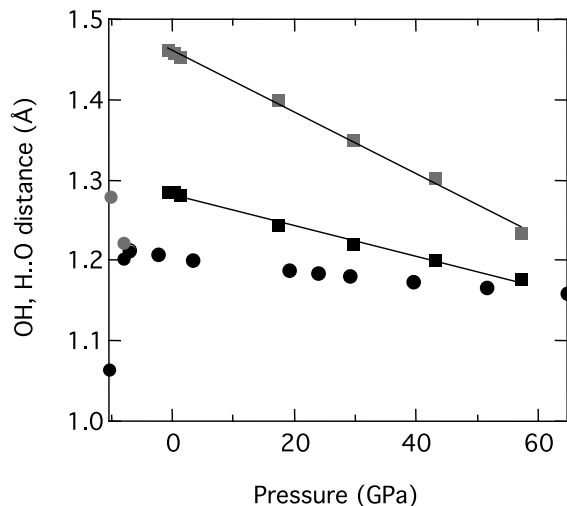


Fig. 3. OH (black) and O..H (gray) distances as a function of pressure in δ -AlOOH (circles) and 4.2 mol% $\text{Al}^{3+}+\text{H}^{+}$ (squares). In δ -AlOOH, at pressures less than -8 GPa (O–O distance of 2.422 Å), the symmetric bond splits into a short OH bond and longer O..H bond. For lower pressures (-10 GPa), the structure degenerates into a triclinic structure.

less than zero), opposite to the trend we predict for δ -AlOOH.

Results for two substitutions show that the enthalpy of solution does not depend strongly on their mutual arrangement: results for edge- and corner-sharing Al-octahedra and maximally separated substitutions differ by less than 0.37 eV at 0 GPa (Fig. 4a). This indicates that the entropy of mixing is nearly ideal, and therefore Eq. 3 applies.

4. Solubility of $\text{Al}^{3+}+\text{H}^{+}$ in stishovite

By comparing to the enthalpies of the end-members, we find that the solid solution has a positive enthalpy of solution. The magnitude of the enthalpy of solution (1.1 eV/defect at 0 GPa; Eq. 5), is small enough to allow significant solution at modest temperatures (Eqs. 1–3) (Fig. 4a). Increasing pressure decreases the enthalpy of solution, which means that we expect the solubility to increase with increasing pressure.

Based on our first principles results and a model for the entropy of solution as discussed above, we find that the solubility of hydrogen and alu-

minum into stishovite at 1500 K and 25 GPa is about 2.0 mol% (0.3 wt% H_2O), increasing to 7.5 mol% (1.15 wt% H_2O) at 60 GPa. Compared to available data from Ono et al. [33] for the breakdown of phase Egg, $\text{AlSiO}_3(\text{OH})$, between 11 and 17 GPa, the predicted solubilities at 0 and 25 GPa bracket these experimental values (Fig. 4b), indicating the coupled $\text{Al}^{3+}+\text{H}^{+}$ substitution is a likely mechanism for water incorporation in stishovite.

Additional arrangements of hydrogen in the

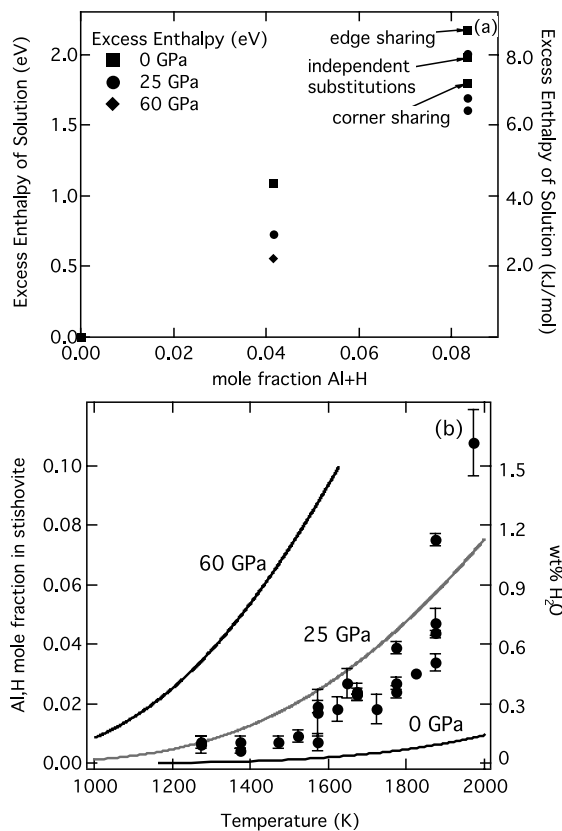


Fig. 4. (a) Enthalpy of solution at 0 GPa (squares), 25 GPa (circles) and 60 GPa (diamonds). With increasing pressure, the enthalpy of solution decreases significantly. Multiple substitutions show small differences as a function of their proximity indicating nearly ideal entropy of mixing. (b) Calculated solubility of aluminum and hydrogen into stishovite as a function of temperature and pressure (0 GPa, lower black curve; 25 GPa, gray curve; 60 GPa, upper black curve) compared to aluminum content in stishovite upon the breakdown of phase Egg [33] between 11 and 17 GPa (circles).

unit cell can also increase the number of possible sites, and therefore increase the configurational entropy contribution to the solubility, though at the cost of a higher enthalpy. As discussed above, additional arrangements tested have a significantly greater energy (> 1 eV) than the lowest energy configuration considered here and so are expected to contribute little to the partition function or the solubility. Calculations show that consideration of these higher-energy arrangements will increase the total solubility, and therefore our results should be considered a lower bound. A single arrangement with 1 eV greater excess enthalpy of mixing contributes an additional solubility of 0.07 mol% Al^{3+} and H^+ in stishovite at 25 GPa and 2000 K (0.9% relative increase).

5. Discussion and conclusions

Our results support the proposed coupled substitution of $\text{Si}^{4+} + \text{O}^{2-} = \text{Al}^{3+} + \text{OH}^-$ in stishovite and find a maximum solubility of 0.3 wt% H_2O in stishovite at 25 GPa and 1500 K. Stishovite forming in subducting slabs [8,34] can be expected to form in the presence of Al and H, incorporating significant amounts of both aluminum and hydrogen. If significant amounts of water exist in oceanic crust subducted to depths greater than 300 km, stishovite must be considered a candidate for crystallographic storage of that water. Significant hydrogen and aluminum solubility in stishovite, also has important implications for our understanding of phase equilibria in subducting slabs; our results and previous experimental results indicate that stishovite cannot be treated as a pure phase in the presence of Al and H. We note that coexisting phases (i.e. perovskite, garnet, corundum) may compete with stishovite for Al and/or H, so that the maximum solubility of Al+H in stishovite in a multi-phase mantle assemblage may be less than we have calculated.

Our results suggest that hydrogen bonding in Earth may not be uniformly asymmetric as is commonly observed in hydrous and nominally anhydrous minerals at low pressure. We find symmetric bonding in the δ -AIOOH end-member at zero pressure. The solid solution shows a ten-

dency towards greater symmetry of the hydrogen bond with increasing pressure; extrapolation of the trends shown in Fig. 3 indicate that the solid solution may exhibit symmetric bonding at a pressure of 93 GPa. Pressure-induced symmetrization of the hydrogen bond would alter much of the physics and chemistry of hydrogen incorporation in minerals, including the elastic constants.

The stishovite- δ -AIOOH solid solution provides a uniquely clear opportunity to investigate the influence of hydrogen on the elasticity of a nominally anhydrous mineral (NAM). In many NAMs, the addition of hydrogen is accompanied by the addition of other impurities or defects that also have a substantial influence on the elasticity, making it difficult to isolate the effect of the hydrogen bond. For instance, well-characterized hydrous ringwoodite samples indicate that hydrogen substitutes directly for Mg^{2+} and Si^{4+} , resulting in a significantly weaker structure [35,36]. In the case of stishovite, the bulk modulus of the defect AlO_6 octahedra (257 GPa [28]) are similar in stiffness to the host SiO_6 octahedra (342 GPa [28]), which, along with the location of the hydrogen bonds in the a - b plane allow us to effectively isolate their influence.

The influence of hydrogen on elasticity depends strongly on whether the hydrogen bond is asymmetric or symmetric; the asymmetric bond appears to influence elastic anisotropy much more strongly than volume compression. The asymmetric hydrogen bond in the solid solution weakens the a - b plane ($K_{c0}/K_{a0} = 1.24$), as compared with the stishovite end-member ($K_{c0}/K_{a0} = 1.4$). The equation of state is not significantly affected: the relative compression as a function of pressure is indistinguishable for solid solution and stishovite, as are best-fit bulk moduli (Table 3). The effect of the hydrogen bond is expected to be qualitatively different above 93 GPa where hydrogen bonding in the solid solution may be symmetric. Here, comparison with the AIOOH end-member suggests that the a - b plane will be stiffened as compared with stishovite. We find that the symmetric bond in δ -AIOOH substantially stiffens the a - b plane with respect to the c -axis. Indeed, the symmetric hydrogen bond is the stiffest bond in the structure with a linear modulus of 1527 GPa, as

compared with that of the Si–O bond in stishovite of 1026 GPa.

The solubility of hydrogen in stishovite increases rapidly with increasing pressure, behavior also found in many low-pressure silicates [5–7]. In the case of stishovite, we may relate the pressure-induced increase in solubility directly to the crystal chemistry of the solid solution. The stishovite– δ -AlOOH join shows a negative volume of solution: the solid solution has a smaller volume than a mechanical mixture of the end-members of the same bulk composition and is therefore increasingly favored with increasing pressure. The thermodynamic relationship between enthalpy and volume of solution, ΔV is:

$$\frac{\partial \Delta H}{\partial P} = \Delta V \quad (13)$$

From the zero pressure volumes listed in Table 1, we find $\Delta V = -0.15 \text{ \AA}^3$, which is indistinguishable within our numerical precision from the value found from inspection of Fig. 4a: $-0.54 \text{ eV}/60 \text{ GPa} = -0.12 \text{ \AA}^3$. We may further relate the negative volume of solution to the crystal structure. We find that the average zero-pressure Al–O bond length in the solid solution (1.83 Å) is substantially less than that in the δ -AlOOH end-member (1.91 Å). We attribute this to the stiffness of the stishovite matrix in which the Al-octahedron is embedded and the small amount of relaxation that occurs about the defect. The relative lack of accommodation is reflected in the value of the relaxation parameter, $\epsilon = 0.47$ [37,38], which is at the low end of what has been observed in other solid solutions. Finally, we note that the mismatch between Al–O and Si–O bond lengths in the solid solution is partly relieved by the presence of H, which lowers the symmetry, allowing the Al-octahedron to rotate.

We speculate that the Al+H for Si substitution may be effective in other octahedrally coordinated silicates, such as Mg-rich silicate perovskite. This suggests that previous results on Al-free compositions [39,40] may not be representative of the ability of perovskite to store water in the lower mantle. However, the energetics of solution in perovskite are considerably richer than they are in stishovite. The energetics of the Al+H for Si

substitution would have to be considered in concert with those of the Tschermak ($\text{Mg}^{2+} + \text{Si}^{4+} = 2\text{Al}^{3+}$) and Brownmillerite substitutions ($2\text{Si}^{4+} + \text{O}^{2-} = 2\text{Al}^{3+} + \text{V}_\text{O}$) [41]. **[SKJ]**.

References

- [1] Q. Williams, R.J. Hemley, Hydrogen in the Deep Earth, Annual Reviews, 2001.
- [2] J. Chen, T. Inoue, D.J. Weidner, W. Yujun, M.T. Vaughan, Strength and water weakening of mantle minerals, olivine, wadsleyite and ringwoodite, Geophys. Res. Lett. 25 (1998) 575–578.
- [3] H. Jung, S. Karato, Water-induced fabric transitions in olivine, Science 293 (2001) 1460–1463.
- [4] D.R. Bell, G.R. Rossman, Water in Earth's mantle – the role of nominally anhydrous minerals, Science 255 (1992) 1391–1397.
- [5] R. Lu, H. Keppler, Water solubility in pyrope to 100 kbar, Contrib. Mineral. Petrol. 129 (1997) 35–42.
- [6] Q. Bai, D.L. Kohlstedt, Substantial hydrogen solubility in olivine and implications for water storage in the mantle, Nature 357 (1992) 672–674.
- [7] D.L. Kohlstedt, H. Keppler, D.C. Rubie, Solubility of water in the α , β and γ phases of $(\text{Mg}, \text{Fe})_2\text{SiO}_4$, Contrib. Mineral. Petrol. 123 (1996) 345–357.
- [8] T. Irifune, A.E. Ringwood, Phase transformations in subducted oceanic crust and buoyancy relationships at depths of 600–800 km in the mantle, Earth Planet. Sci. Lett. 117 (1993) 101–110.
- [9] S. Kesson, J. Fitz Gerald, J.M.G. Shelley, Mineral chemistry and density of subducted basaltic crust at lower-mantle pressures, Nature 372 (1994) 767–769.
- [10] W.R. Panero, L.R. Benedetti, R. Jeanloz, Equation of state of stishovite and interpretation of SiO_2 shock-compression data, J. Geophys. Res. 108 (B1) (2003), doi:10.1029/2001JB001663.
- [11] S. Ono, T. Suto, K. Hirose, Y. Kuwayama, T. Komabayashi, T. Kikegawa, Equation of state of Al-bearing stishovite to 40 GPa at 300 K, Am. Mineral. 87 (2002) 1486.
- [12] A.R. Pawley, P.F. McMillan, J.R. Holloway, Hydrogen in stishovite, with implications for mantle water content, Science 261 (1993) 1024–1026.
- [13] W.R. Panero, L.R. Benedetti, R. Jeanloz, Transport of water into the lower mantle: Role of stishovite, J. Geophys. Res. 108 (B1) (2003), doi:10.1029/2002JB002053.
- [14] E. Ohtani, K. Litasov, A. Suzuki, T. Kondo, Stability field of new hydrous phase, δ -AlOOH, with implications for water transport into the deep mantle, Geophys. Res. Lett. 28 (2001) 3991–3993.
- [15] E. Wolanin, P. Pruzan, J.C. Chervin, B. Canny, M. Gauthier, D. Hausermann, M. Hanfland, Equation of state of ice VII up to 106 GPa, Phys. Rev. B 56 (1997) 5781–5785.

- [16] H.S.C. O'Neill, A. Navrotsky, Cation distributions and thermodynamic properties of binary spinel solid solutions, *Am. Mineral.* 69 (1984) 733–753.
- [17] G. Kresse, J. Furthmüller, Efficiency of ab-initio total energy calculations for metals and semiconductors, *Comput. Mater. Sci.* 6 (1996) 15–50.
- [18] G. Kresse, J. Furthmüller, Efficient iterative schemes for ab initio total-energy calculations using a plane-wave basis set, *Phys. Rev. B* 54 (1996) 11169–11186.
- [19] G. Kresse, J. Hafner, Ab initio molecular-dynamics for liquid-metals, *Phys. Rev. B* 47 (1993) 558–561.
- [20] G. Kresse, J. Hafner, R.J. Needs, Optimized norm-conserving pseudopotentials, *J. Phys. Condens. Matter* 4 (1992) 7461–7468.
- [21] D. Andrault, C. Fiquet, F. Guyot, M. Hanfland, Pressure-induced Landau-type transition in stishovite, *Science* 282 (1998) 720–724.
- [22] B.B. Karki, L. Stixrude, J. Crain, Ab initio elasticity of three high-pressure polymorphs of silica, *Geophys. Res. Lett.* 24 (1997) 3269–3272.
- [23] A. Suzuki, E. Ohtani, T. Kamada, A new hydrous phase δ -AlOOH synthesized at 21 GPa and 1000°C, *Phys. Chem. Miner.* 27 (2000) 689–693.
- [24] T. Fujihara, M. Ichikawa, T. Gustafsson, I. Olovsson, T. Tsuchida, Powder-neutron diffraction studies of geometric isotope and hydrogen-bonding effects in β -CrOOH, *J. Phys. Chem. Solids* 63 (2002) 309–315.
- [25] J. Aidun, M.S.T. Bukowinski, M. Ross, Equation of state and metallization of CsI, *Phys. Rev. B* 29 (1984) 2611–2621.
- [26] H. Wanatabe, Thermochemical properties of synthetic high-pressure compounds relevant to the Earth's mantle, in: S. Akimoto, M.H. Manghni (Eds.), *High Pressure Research in Geophysics 12*, Center for Academic Publications, Tokyo, 1982, pp. 441–464.
- [27] O.L. Anderson, D.G. Isaak, Elastic constants of mantle minerals at high temperature, in: T.J. Ahrens (Ed.), *Mineral Physics and Crystallography: A Handbook of Physical Constants*, AGU Reference Shelf 2, American Geophysical Union, 1995.
- [28] N.L. Ross, J.F. Shu, R.M. Hazen, T. Gasparik, High-pressure crystal chemistry of stishovite, *Am. Mineral.* 75 (1990) 739–741.
- [29] J. Tsuchiya, T. Tsuchiya, S. Tsuneyuki, T. Yamanaka, First principles calculation of a high-pressure hydrous phase, δ -AlOOH, *Geophys. Res. Lett.* 29 (19) (2002), doi:10.1029/2002GL015417.
- [30] C.B. Vanpeteghem, E. Ohtani, T. Kondo, Equation of state of the hydrous phase δ -AlOOH at room temperature up to 22.5 GPa, *Geophys. Res. Lett.* 29 (2002) 014224.
- [31] N.L. Ross, G.V. Gibbs, K.M. Rosso, Potential docking sites and positions of hydrogen in high-pressure silicates, *Am. Mineral.* (2003) (in press).
- [32] S.K. Sikka, Hydrogen bonding under pressure, *Indian J. Pure Appl. Phys.* 35 (1997) 677–681.
- [33] S. Ono, High temperature stability limit of phase egg, $\text{AlSiO}_3(\text{OH})$, *Contrib. Mineral. Petrol.* 137 (1999) 83–89.
- [34] M.W. Schmidt, S. Poli, Experimentally based water budgets for dehydrating slabs and consequences for arc magma generation, *Earth Planet. Sci. Lett.* 163 (1998) 361–379.
- [35] H. Yusa, T. Inoue, Y. Ohishi, Isothermal compressibility of hydrous ringwoodite and its relation to the mantle discontinuities, *Geophys. Res. Lett.* 27 (2000) 413–416.
- [36] T. Inoue, D.J. Weidner, P.A. Northrup, J.B. Parise, Elastic properties of hydrous ringwoodite (γ -phase) in Mg_2SiO_4 , *Earth Planet. Sci. Lett.* 160 (1998) 107–113.
- [37] J.L. Martins, A. Zunger, Bond lengths around isovalent impurities and in semiconductor solid solutions, *Phys. Rev. B* 30 (1984) 6217–6220.
- [38] Y.J. Lee, R.J. Reeder, R.W. Wenskus, E.J. Elzinga, Structural relaxation in the MnCO_3 – CaCO_3 solid solution: a Mn K-edge EXAFS study, *Phys. Chem. Miner.* 29 (2002) 585–594.
- [39] N. Bolfan-Casanova, H. Keppler, D.C. Rubie, Water partitioning between nominally anhydrous minerals in the MgO – SiO_2 – H_2O system up to 24 GPa implications for the distribution of water in the Earth's mantle, *Earth Planet. Sci. Lett.* 182 (2000) 209–221.
- [40] C. Meade, J.A. Reffner, E. Ito, Synchrotron infrared absorbance measurements of hydrogen in MgSiO_3 perovskite, *Science* 264 (1994) 1558–1560.
- [41] A. Navrotsky, M. Schoenitz, H. Kojitani, H. Xu, J. Zhang, D.J. Weidner, R. Jeanloz, Aluminum in magnesium silicate perovskite: Formation, structure, and energetics of magnesium-rich defect solid solutions, *J. Geophys. Res.* 108 (B7) (2003), doi:10.1029/2002JB002055.